Clinical Immunology 283 (2026) 110656

Contents lists available at ScienceDirect

Clinical Immunology

journal homepage: www.elsevier.com/locate/yclim

Full Length Article

Long-term immune and epigenetic dysregulation following COVID-19

Chrysanthi Sidiropoulou [a], Garyphallia Poulakou [b], Evdoxia Kyriazopoulou [c], Elisavet Tasouli [d], Efthymia Giannitsioti [e], Anna Strikou [f], Maria Tsilika [g], Eirini Christaki [h], Vassiliki Rapti [b], Vassiliki Evangelopoulou [g], Nikoletta Rovina [i], Nathalie Iannotti [j], Emanuele Nicastri [k], Eleonora Taddei [l], Helena Florou [g], Andrea Angheben [m], Matteo Bassetti [n], Lorenzo Dagna [o,aa], Antonio Torres [p], Spyros Foutadakis [g], George Adamis [q], Emmanouil Stylianakis [g], Giannis Vatsellas [r], Georgia Damoraki [c], Leda Efstratiou [g], Christina Damoulari [c], Konstantinos Leventogiannis [c], Achilleas Laskaratos [c], Panagiotis Koufargyris [c], Nikoletta Charalampaki [c], Paraskevi Chra [c], Aglaia Galanopoulou [c], Dimitris Thanos [r], Periklis Panagopoulos [s], Konstantinos Syrigos [b], Athanasios Ziogas [t], Rob ter Horst [t,u], Jos W.M. van der Meer [t], Konstantina Iliopoulou [v], Francesco Saverio Serino [w], Maria Pavlaki [x], Pierluigi Del Vecchio [l], Laura Scorzolini [k], Alessandra Bandera [j], Agamemnon Bakakos [y], Styliani Sympardi [d], Haralampos Milionis [h], Mihai G. Netea [t,z], Evangelos J. Giamarellos-Bourboulis [c,g,*]

[a] 2nd Department of Internal Medicine, Tzaneio General Hospital of Piraeus, Piraeus, Greece
[b] 3rd Department of Internal Medicine, National and Kapodistrian University of Athens, Medical School, Greece
[c] 4th Department of Internal Medicine, National and Kapodistrian University of Athens, Medical School, Greece
[d] 1st Department of Internal Medicine, Thriasio General Hospital of Elefsis, Elefsis, Greece
[e] 1st Department of Propedeutic Medicine, Laikon Athens General Hospital, Athens, Greece
[f] HIV Infection Unit, Andreas Syggros Hospital, Athens, Greece
[g] Hellenic Institute for the Study of Sepsis, Athens, Greece
[h] 1st Department of Internal Medicine, University of Ioannina, Medical School, Ioannina, Greece
[i] 2nd Department of Pulmonary Medicine, "Sotiria" Athens General Hospital of Chest Diseases, Athens, Greece
[j] Infectious Diseases Unit, Foundation IRCCS Ca' Granda Ospedale Maggiore Policlinico, Department of Pathophysiology and Transplantation, University of Milan, Milan, Italy
[k] High Isolation Infectious Diseases Unit, National Institute for Infectious Diseases 'Lazzaro Spallanzani' IRCCS, Rome, Italy
[l] Dipartimento Scienze di Laboratorio e Infettivologiche - Fondazione Policlinico Gemelli IRCCS, Roma, Italy
[m] Department of Infectious, Tropical Diseases & Microbiology, IRCCS Sacro Cuore Don Calabria Hospital, Negrar di Valpolicella, Verona, Italy
[n] Infectious Disease Clinic, Department of Health Sciences, Ospedale Policlinico San Martino IRCCS, University of Genoa, Genoa, Italy
[o] Unit of Immunology, Rheumatology, Allergy and Rare Diseases (UniRAR), IRCCS San Raffaele Scientific Institute, Milano, Italy
[p] Pulmonary Department, Hospital Clinic, Universitat de Barcelona, IDIBAPS, ICREA, Barcelona, Spain
[q] 1st Department of Internal Medicine, "G.Gennimatas" Athens General Hospital, Athens, Greece
[r] Center of Basic Research, Biomedical Research Foundation, Academy of Athens, Athens, Greece
[s] 2nd Department of Internal Medicine, Dimocritus University of Thrace, Medical School, Alexandroupolis, Greece
[t] Department of Internal Medicine and Radboud Center for Infectious Diseases, Radboud University, Nijmegen, the Netherlands
[u] CEMM, Vienna, Austria
[v] 2nd Department of Internal Medicine, Thriasio General Hospital of Elefsis, Elefsis, Greece
[w] Department of Internal Medicine, Hospital of Jesolo, Jesolo, Italy
[x] Department of Internal Medicine, General Hospital of Argolida, Argos, Greece
[y] 1st Department of Pulmonary Medicine, National and Kapodistrian University of Athens, Medical School, Greece
[z] Department of Immunology and Metabolism, Life and Medical Sciences Institute, University of Bonn, Germany
[aa] Vita-Salute San Raffaele University, 20132 Milano, Italy

* Corresponding author at: 4th Department of Internal Medicine, National and Kapodistrian University of Athens, Medical School, Greece.
E-mail address: egiamarel@med.uoa.gr (E.J. Giamarellos-Bourboulis).

https://doi.org/10.1016/j.clim.2025.110656
Received 7 October 2025; Received in revised form 30 November 2025; Accepted 9 December 2025
Available online 13 December 2025

ARTICLE INFO

Keywords:
Post-acute COVID-19 syndrome (PACS)
Phenotypes
Immune dysregulation
IL-1
Cytokines
Lung function tests

ABSTRACT

Post-Acute COVID-19 syndrome (PACS) is heterogeneous in phenotype and functional state. This prospective, observational study studied adults six months after acute COVID-19. We defined clinical phenotypes and profiled plasma mediators grouped into functional pathways (IL-1, IL-17, IFNγ/IFNγ-related cytokines, pro−/anti-inflammatory clusters). A subset underwent RNA-seq and ChIP-seq experiments. Three cohorts were analyzed (Exploratory $n = 46$; Discovery $n = 591$; Validation Cohort $n = 289$). PACS compatible symptoms were identified in 69.6 %; 59.2 % and 54.7 % respectively. Five phenotypes emerged. IL-1 cytokines (OR: 3.17, 95 % CIs: 1.94–5.19, p: 4.5×10^{-6}), IL-17 cytokines (OR: 2.45, 95 % CIs: 1.47–4.07 p: 5.88×10^{-4}) and the anti-inflammatory biomarkers (OR: 2.15, 95 % CIs: 1.34–3.45, p: 1.5×10^{-3}) were upregulated in PACS patients. Respiratory phenotype was correlated with IL-1 upregulation (OR 4.23; 95 % CIs, 1.69–10.8, $p = 0.0025$). Transcriptomic and epigenomic changes were observed. Distinct phenotypes of PACS are driven by different immunological mechanisms at the DNA, transcriptomic, and protein levels.

1. Introduction

Post-Acute COVID-19 syndrome (PACS) - also described as "Long COVID", is characterized by significant heterogeneity regarding phenotypes and immune function. The consensus definition by patients, clinicians, researchers, and WHO suggests that PACS usually occurs within 3 months upon acute infection and is characterized by at least 2-month-lasting symptoms that cannot be explained by other diagnoses. Common symptoms include fatigue, shortness of breath, and cognitive dysfunction. These symptoms may start following recovery from acute COVID-19 or persist after cessation of acute illness [1]. Inappropriate activation of innate and adaptive immune responses has been suggested to play a central role in the pathogenesis of PACS [2].

There is no consensus regarding the incidence of PACS, but it has been reported to develop in up to 10–20 % of COVID-19 cases, with a rough global estimate of 50 million individuals [3]. In a recent meta-analysis of 1.2 million patients from 22 countries, respiratory symptoms were prevailing, affecting 33.4 % of COVID-19 survivors and represented a major cause of morbidity and disability [4].

In light of the clinical heterogeneity observed, classification of PACS patients into phenotypes and association with immune and organ function is crucial. This may also guide the development of new therapies. In this study we systematically investigate the immunological signatures underlying the diverse clinical phenotypes observed in PACS. Given the clinical heterogeneity of PACS, we aimed to determine whether distinct patterns of immune dysregulation are associated with specific clinical phenotypes. Finally, for a subset of patients, we performed RNA-seq and H3K27ac ChIP-seq experiments to identify whether alterations in transcriptomic and epigenomic landscapes may accompany changes in cytokine production.

2. Methods and materials

2.1. Study design and patient cohorts

This is a prospective, observational study conducted in outpatient post COVID units in Greece (five sites), Italy (eight sites) and Spain (one site). The first part of the study of 2020 was run under approval of the protocol ESCAPE (EudraCT number 2020–001039-29; Clinicaltrials.gov NCT04339712); the remaining study run under approvals by the Ethics Committee of the participating hospitals (Attikon University Hospital 11/1/2022; General Hospital of Piraeus Tzaneio 14/5/2021; Sotiria General Hospital of Chest Diseases-3rd University Department of Internal Medicine 28/3/2022; Sotiria General Hospital of Chest Diseases-1st University Pulmonary Medicine Department 28/3/2022, Thriasio General Hospital 13/4/2022; Ospedale Policlinico San Martino 2/5/2022; IRCCS Lazzaro Spallanzani 14/7/2022; Policlinico Universitario Agostino Gemelli 3/3/2022; Spedali civili 5/4/2022; Ospedale Sacro Cuore Don Calabria 23/2/2022; IRCCS San Raffaele 11/5/2022; Ospedale di Jesolo-Unità Operativa Malattie Infettive 15/3/2022; Ospedale Maggiore Policlinico 12/4/2022; Hospital Clínic de Barcelona 10/6/2022). The laboratory of Immunology of Infectious Diseases of the 4th Department of Internal Medicine at ATTIKON University General Hospital served as the central laboratory.

Adult patients were enrolled six months after acute COVID-19 infection. At the time of inclusion, the patients had negative molecular tests for SARS-CoV-2 (Cobas SARS-COV-2 RT-PCR, Roche Diagnostics). Exclusion criteria were: a) any stage IV malignancy; b) any primary immunodeficiency; c) neutropenia with fewer than 1.500 neutrophils per mm^3; d) oral or intravenous intake of corticosteroids at a daily dose greater than or equal to 0·4 mg kg^{-1} of prednisone or equivalent for a period longer than 15 consecutive days in the last 3 months; and e) any chronic anti-cytokine biological treatment. For all patients, the following information was documented: date of COVID-19 infection, severity of disease, need for hospitalization and/or admission in Intensive Care Unit (ICU), demographics (age, sex) and Charlson's comorbidity index (CCI).

The study included both male and female participants. Sex distribution was documented in all cohorts and comparisons between sex-matched patients and controls were analyzed. The study was not limited to a single sex; thus the results are expected to be relevant for both sexes.

Patients were divided into three cohorts. The Exploratory Cohort was recruited from one study site, between September and October 2020 and included 46 patients; they were compared with 25 sex- and age-matched controls without a history of COVID-19 infection and negative anti-SARS-CoV-2 antibodies. Patients who were recruited from June 2021 to August 2023 were randomly 2:1 split into two cohorts; the Discovery Cohort and the Validation Cohort. Healthy asymptomatic vaccinated comparators were also enrolled.

2.2. Questionnaires and functional tests

PACS was defined according to the WHO consensus definition[1] as symptoms that lasted for at least 2 months which could not be explained by an alternative diagnosis and occured within 3 months after the acute COVID-19 infection. The discrimination of specific clinical phenotypes was accomplished using an electronic 16-symptoms questionnaire to be answered as either Yes or No. This questionnaire was developed by the researchers as a tool to assess quality of life and was already used in the SAVE-MORE trial [5]. Patients with at least one positive response to the 16-symptoms questionnaire were considered to suffer from PACS. For further validation of our classification, we used the Symptom Tool-Impact Tool (ST-IT) questionnaire which is internationally proposed for follow-up of COVID-19 patients [6]; the Short Form (SF)-36 health survey and we also assessed the respiratory status of patients by performing spirometry, plethysmography and carbon monoxide diffusing capacity (DL_{CO} Elite Series Plethysmograph, Medical Graphics, Minnesota, USA). Forced expiratory volume in one minute (FEV_1), forced vital capacity (FVC), FEV_1/FVC ratio, total lung capacity (TLC) and diffusing

capacity for carbon monoxide were performed and evaluated by the same pulmonologist (VE) to limit bias. Pulmonary function tests were considered abnormal with any decrease of $DL_{CO} < 76$ % or a decrease of TLC <80 % and/or FEV1/FVC <0.7. To exclude an alternative diagnosis, patients underwent thorough clinical, laboratory and radiological evaluation by their attending physicians

2.3. Cytokine assays

A blood sample of 20 ml was drawn from a peripheral forearm vein under aseptic conditions. The samples were collected into a) tubes with ethylenediaminetetraacetic acid (EDTA) and transferred within one hour to the central laboratory for isolation and culture of peripheral blood mononuclear cells (PBMCs) and b) in sterile pyrogen-free tubes for serum collection. Similar blood sampling was performed in comparators without a known history of COVID-19 infection, irrespective of vaccination status and matched for age, sex and Charlson's comorbidity index (CCI). PBMCs were isolated using gradient centrifugation over a Ficoll-Hypaque density gradient (Biochrom, Berlin, Germany) after 1400 *g* at 4 °C centrifugation for 25 min. After three washings in ice-cold PBS (phosphate buffered saline, pH: 7.2, Biowest, France), PBMCs were counted using a Neubauer plate with trypan blue exclusion of dead cells. PBMCs were incubated in 1 ml RPMI 1640 (Biochrom, Berlin, Germany) supplemented with 100 U/ml penicillin G and 0.1 mg/ml streptomycin and distributed on 96-well plates at a final volume of 200 μl and density 5×10^6/ml. Cells were incubated at 37°C and 5 % CO_2 for 24 hours without/with 10 ng/ml lipopolysaccharide (LPS) of *Escherichia coli* O55: B5. Cells were also incubated in same conditions for five days with 10 % fetal bovine serum without/with 5×10^6 cfu/ml heat-killed *Candida albicans* (HKCA). After incubation the supernatants were collected. The cell pellet was treated with Triton X-100 and IL-1α was measured in supernatants by an enzyme immunosorbent assay. CRP, troponin, NT-proBNP were measured with an immuno-chemiluminometric assay (ADVIA 1800/ ADVIA 2400, Siemens Healthineers Laboratory Diagnostics, USA) in plasma.

Cytokines and inflammatory mediators were measured in plasma and cell supernatants by enzyme immunosorbent assays. Lower detection limits were: for CRP 0.5 mg/l; for troponin I 2 ng/l; for NT-proBNP 35 pg/ml; for IL-1ra and S100A8/A9 31 pg/ml; for TNF 20 pg/ml; for FGF23 156 pg/ml; for IL-1β and IL-1α 10 pg/ml; for IL-6 40 pg/ml; for IL-10 25 pg/ml; for IL-17 A 8 pg/ml; for IL-22 16 pg/ml; for IL-33R 1565 pg/ml; for IFNγ 78 pg/ml; for IP-10 63 pg/ml; for MMP-9 16 ng/ml; for PDGF-A 312 pg/ml; for sgp130 15·5 ng/ml; for s-Selectin 15 ng/ml; for S100A8/A9 63 ng/ml.

2.4. RNA-seq experiments

Total RNA was isolated from whole blood stored in PAXgene® Blood RNA Tubes using the QIAsymphony PAXgene® Blood RNA kit. Sequencing libraries were prepared using the NebNext Ultra II Directional RNA kit. Library quality was examined using an Agilent 2100 Bioanalyzer, and libraries were quantified with a Qubit fluorometer. Samples were sequenced in a single-end mode using a Novaseq 6000 sequencer at the Greek Genome Center situated at the Biomedical Research Foundation Academy of Athens (BRFAA).

2.5. ChIP-seq experiments

Samples were prepared for ChIP-seq using a previously published protocol [7] with modifications. Briefly, approximately 4 million PBMCs per sample were fixed with 1 % formaldehyde for 30 minutes at room temperature and quenched with 0.125 M glycine for 5 minutes. Following cell and nuclei lysis, chromatin was sonicated using a Covaris S220 instrument. For the immunoprecipitation step chromatin was incubated overnight with 6 μl of H3K27ac antibody (Cell Signaling, #4353). Following immobilization on protein G beads and washing steps, samples were treated with proteinase K, and crosslinks were reversed overnight at 65 °C and the DNA was purified with Nucleomag beads. Libraries were prepared using the NEBNext® Ultra™ II DNA Library Prep Kit for Illumina. DNA concentration was measured with a Qubit fluorometer, and library sizes were assessed using the Agilent 2100 Bioanalyzer instrument. Samples were sequenced in a NovaSeq 6000 Illumina sequencer at the Greek Genome Center situated at BRFAA.

2.6. Statistical analysis

Categorical data were presented as frequencies and confidence intervals (CIs); continuous variables with normal distribution as mean with standard deviation (SD) and data with non-normal distribution as median with interquartile range. Fisher's exact test was used for the comparison of categorical data; Student's *t*-test or non-parametric Mann-Whitney *U* test were used for the comparison of continuous data, as appropriate. Clustering of symptoms was done between patients providing at least one positive reply to the developed 16-element questionnaire followed by Principal Component Analysis (PCA). Abnormal pulmonary function tests were considered the gold-standard for the diagnosis of predominant respiratory phenotype. For patients missing pulmonary function tests, clinical answers to the questionnaires reported by patients with abnormal pulmonary function tests were used to extrapolate classification into respiratory PACS. More precisely, positive questions were compared by chi-square to define those associated with abnormal pulmonary function tests.

Patients and healthy comparators were grouped into five groups of cytokines, IL-1 cytokines; IFNγ-related cytokines; IL-17 cytokines; anti-inflammatory meditators; and pro-inflammatory mediators. To achieve so, the median of distribution of each cytokine was determined and patients were considered scoring positive for each of the cytokines when above the median. The IL-1 cytokines group included IL-1β, IL-1α, and IL-1ra in the supernatants of PBMCs, and plasma IL-1ra and IL-18. IFNγ-related cytokines group included plasma IFNγ, IP-10, CXCL9, IL-8 and IFNγ in the supernatants of PBMCs. IL-17 group included plasma IL-17, and IL-17 in the supernatants of PBMCs. Anti-inflammatory mediators included plasma TGFb, FGF23, PDGF-A and S100A8/A9. Pro-inflammatory mediators included plasma CRP, ferritin, IL-6, IL-10, sCD163, sgp130 and IL-6 and TNFα in the supernatants of PBMCs. Comparisons of the total scores between patients and comparators for each group was done by ordinal regression analysis providing odds ratio (OR) and 95 % confidence intervals (CIs). Any two-sided *p* value lower than 0.05 was considered statistically significant. Statistical analysis was performed using the software IBM SPSS version 26.0.

2.7. RNA-seq analysis

Bioinformatics analyses were performed using the Galaxy Suite [7] and RStudio v2024.04.2 [8] using the R programming language (v4.4.0). The quality of sequencing reads was examined using the FastQC algorithm. Sequencing reads were mapped to the human genome (hg19 version) using HISAT2 [9]. Reads inside genes were calculated with HT-seq count [10], while differential gene expression analysis was performed with DESeq2 [11] using a log2fold change cut-off of 0.5 and adjusted *p* values with a false discovery rate (FDR) < 0.05. Genes with more than 10 counts in ~20 % of the samples were kept for the downstream analysis. Gender information was also included in the DESeq2 model apart from the phenotype. Outlier detection was performed with PCA after variance stabilization with the vst() function from DESeq2. Graphs were produced with the ggplot2 package. GSEA analysis was performed using the WebGestalt software and the KEGG database [12]. Using the DESeq2 output, genes were sorted based on the log2fold-change*(−log10pvalue) metric in preparation for GSEA analysis.

2.8. ChIP-seq analysis

For H3K27ac ChIP-seq, bioinformatics analyses were performed using the Galaxy suite [7]. The quality of the sequencing reads was evaluated using the FastQC algorithm. Sequencing reads were mapped to the hg19 version of the human genome using the Bowtie2 algorithm with the very sensitive end-to-end option [13]. Duplicates were removed using the RmDup command from Samtools [14]. Peaks were called using the MACS2 algorithm with a *p*-value cut-off of 0.05 [15]. All peaks from the different samples were merged into a combined list in preparation for differential analysis. The MultiCovBed command from Bedtools [16] was used to calculate reads for each sample that are contained in the

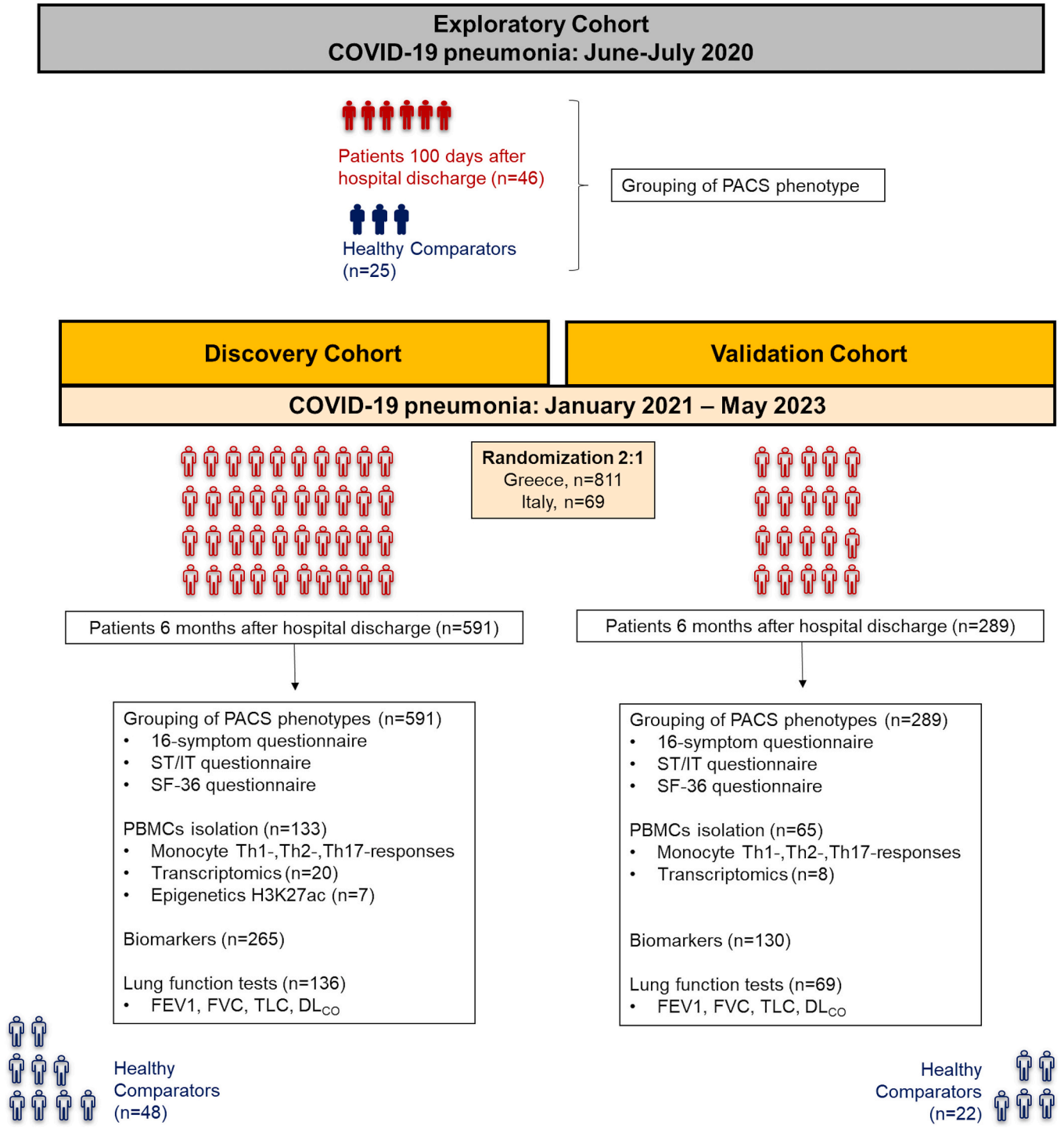

Fig. 1. Study flow chart. The Exploratory Cohort included 46 patients sampled 100 days from hospital discharge and 25 matched comparators. The Discovery Cohort included 591 patients who were evaluated for their symptoms six months after acute COVID-19 disease. Several patients were further sampled for immune function and subjected to lung function tests. 48 matched comparators were also studied. The Validation Cohort included 289 patients who were admitted to an out-patient infectious diseases unit for follow-up and who were evaluated for their symptoms six months post-acute infection; they were matched with 22 healthy comparators. Abbreviations: DL_{CO}: carbon monoxide lung diffusion; FEV1: forced expiratory volume in one second; FVC: forced vital capacity; TLC: total lung capacity; PACS: post-acute COVID syndrome; PBMCs: peripheral mononuclear blood cells; SF-36: Short Form 36 health survey; ST-IT: Symptom Tool-Impact Tool for Long Covid Syndrome.

combined list of peaks. Differential peaks between groups were calculated with the DESeq2 algorithm [11] using as a cut-off a log2foldchange of 0.4, a p-value of 0.05 and a minimum count of 20 reads. Bigwig files were constructed using the bamCoverage command from the Deeptools suite [17]. Heatmaps were prepared with the Morpheus software. Gene ontologies for the closest genes to differential peaks were found using the GREAT tool [18] with the single closest gene (1000 kb) option. The genomic distribution of peaks was calculated using the CEAS software from Cistrome [19,20]. Motif analysis was performed using MEME-ChIP [21]. Since H3K27ac marks the flanking nucleosomes of enhancers and not the core DNA sequence where most transcription factors bind, we constructed a compendium of DNaseI-seq accessible sites marking the core of enhancers from publicly available experiments performed in B cells, T cells, NK cells, monocytes and dendritic cells. DNaseI-peaks were downloaded from the Cistrome Data Browser [22], merged and intersected with the H3K27ac peaks to derive the final list of accessible sites used for motif analysis.

3. Results

3.1. Study flow

The Exploratory Cohort included 46 unvaccinated patients (62.2 % male) and 25 unvaccinated healthy comparators with matched sex and CCI. The Discovery Cohort included 591 patients (47.7 % vaccinated with at least one dose), and the Validation Cohort included 289 patients (56.3 % vaccinated with at least one dose), with 48 and 22 healthy comparators respectively (Fig. 1). Demographic data and comorbidities are shown in Supplementary Tables 1 and 2.

3.2. PACS phenotypes

In the Exploratory Cohort of 46 patients, 32 patients (69.6 %) had signs compatible with PACS and all others had fully recovered. From the Discovery Cohort, 350 patients (59.2; 95 % CIs 55.2 to 63.1 %) were classified as having symptoms compatible with PACS. In the Validation Cohort, 158 patients (54.7 %; 95 % CIs 48.9 to 60.3 %) were classified as PACS (p: 0.22 between Cohorts).

Further clustering into PACS phenotypes was achieved using the 16-element questionnaire (Supplementary Table 3). In the Exploratory Cohort of 32 PACS patients, 24 patients (52.2 %) were reporting fatigue and another eight patients (17.4 %) had predominantly respiratory-compatible symptoms (Supplementary Figure. 1). In the Discovery cohort, five clusters were identified: a) patients with predominantly neurological symptoms (i.e. brain fog, memory problems); b) patients with predominant fatigue; c) patients with mixed fatigue and neurological symptoms; d) patients with mixed respiratory and neurological symptoms; and e) patients with mixed respiratory, neurological and fatigue symptoms (Fig. 2). Similar clustering was identified in the Validation Cohort. We validated the phenotype clustering using the answers provided to the SF-36 and the ST/IT questionnaires (Supplementary Figure. 2).

Patients with prevailing respiratory symptoms had a significantly higher frequency of abnormal TLC and/or DL_{CO} values compared to patients reporting other symptoms; this was observed both in the Discovery and in the Validation Cohorts (Supplementary Figure. 3). The clinical questions that were positively associated with abnormal DL_{CO} values were: “need for rest while doing a daily activity” ($p = 0.002$), “difficulty at work” ($p < 0.0001$), “difficulty in climbing stairs” ($p < 0.0001$), and the “presence of dyspnoea” ($p = 0.027$) (Supplementary Tables 4, 5, 6, and 7). Abnormal TLC values were positively associated with positive answers for “assistance in daily life” and “help to bathe or dress” with a p value of <0.0001 and 0.002, respectively (Supplementary Tables 8, 9). Patients with at least two positive answers to these clinical questions were considered as having a predominantly respiratory phenotype of PACS.

The incidence of respiratory PACS was 14.9 % (88 out of 591 patients; 95 % CIs 12.3 to 17.9) in the Discovery Cohort and 16.2 % (47 out

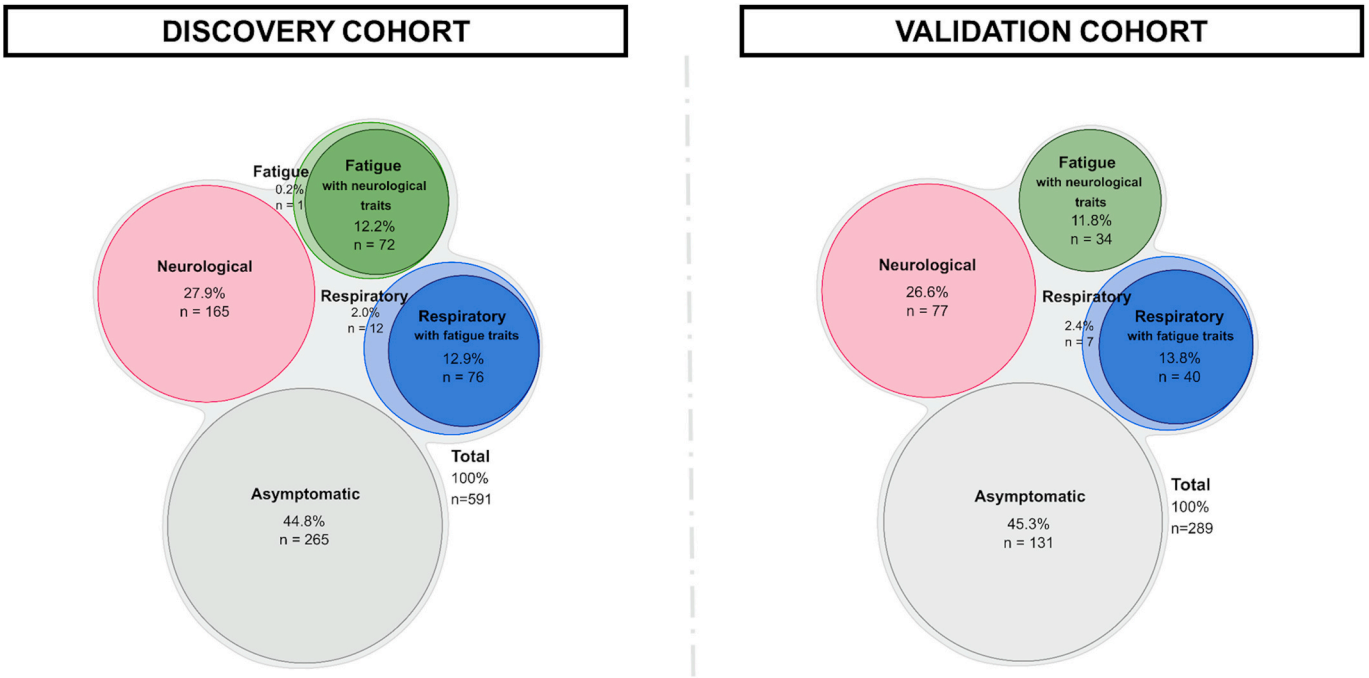

Fig. 2. Phenotype clusters in patients with post-acute COVID syndrome (PACS). Main clusters of symptoms among patients of the Discovery and Validation Cohorts using the 16-element questionnaire, the SF-36 health survey and the ST-IT questionnaire. A negative answer to all of the questions of the 16-element questionnaire is classified as asymptomatic. The respiratory cluster is composed by those patients with either abnormal DL_{CO} and/or TLC. In case lung function tests were not performed, patients that provided at least two positive answers in either of the following: 1) need to rest during an activity; 2) difficulty in manual work; 3) difficulty in climbing stairs and 4) presence of dyspnea or b) two positive answers in both of: 1) need for assistance in everyday activities and 2) difficulty to bath or dress, were classified to the respiratory phenotype. The fatigue cluster was validated by the respective domains of the SF-36 and the ST-IT questionnaires. Abbreviations: SF-36, short form 36 health survey; ST-IT, Symptom Tool-Impact Tool for Long COVID Syndrome; DL_{CO}, carbon monoxide lung diffusion; TLC, total lung capacity.

of 289 patients; 95 % Cis 12.5 to 20.9) in the Validation Cohort ($p = 0.619$). Male patients were less likely to experience respiratory symptoms of PACS than female ($p < 0.0001$), while patients treated with anakinra and dexamethasone during acute infection experienced a lower likelihood for respiratory PACS ($p < 0.0001$) (Supplementary Tables 10, 11 and 12). No other differences regarding demographic data, comorbidities and data from acute infection were observed.

3.3. Inflammatory mediators in PACS patients

Next, we assessed the immune profiles in both the patients of the Discovery and the Validation Cohorts by quantifying circulating plasma cytokines and mediators and evaluating PBMCs cytokine production capacity. In order to investigate the cytokine patterns associated with PACS, we compared the number of cytokines above the median within each cytokine group between PACS patients and healthy comparators. PACS patients exhibited consistent upregulation of the IL-1 cytokines group (OR: 3.17, 95 % CIs: 1.94–5.19, $p = 4.5 \times 10^{-6}$), the IL-17 cytokines group (OR: 2.45, 95 % CIs: 1.47–4.07, $p = 5.88 \times 10^{-4}$) and the anti-inflammatory biomarkers group (OR: 2.15, 95 % CIs: 1.34–3.45, $p = 1.5 \times 10^{-3}$) concomitant with downregulation of the pro-inflammatory biomarkers group (OR:1.92, 95 % CIs: 1.21–3.05, $p = 5.2 \times 10^{-3}$) (Fig. 3).

3.4. Inflammatory mediators in respiratory PACS phenotypes

Since patients with respiratory PACS are a major phenotype, we asked if these patients have any specific immunological modulation. Indeed, we noted hyperactivation of the IL-1 cytokine group in respiratory PACS (OR 4.23; 95 % CIs, 1.69–10.8, $p = 0.0025$) (Supplementary Table 13). We then examined individual mediators and cytokines produced by stimulated PBMCs in order to investigate this signal: patients with respiratory phenotype had also lower concentration of the anti-inflammatory IL-33R ($p = 0.0238$) and significant differences in plasma IFNγ ($p = 0.0002$), IL-6 ($p = 0.048$), FGF23 ($p = 0.0037$) and IP-10 ($p = 0.0019$), along with increased TNFα responses of PBMCs to stimulation with LPS and HCKA ($p = 0.0498$ and 0.0059) and lower IL-10 after HKCA stimulation ($p = 0.0124$). No other difference was observed in levels of plasma mediators and cytokines produced by PBMCs of patients experiencing respiratory symptoms compared with other phenotypes (Fig. 4).

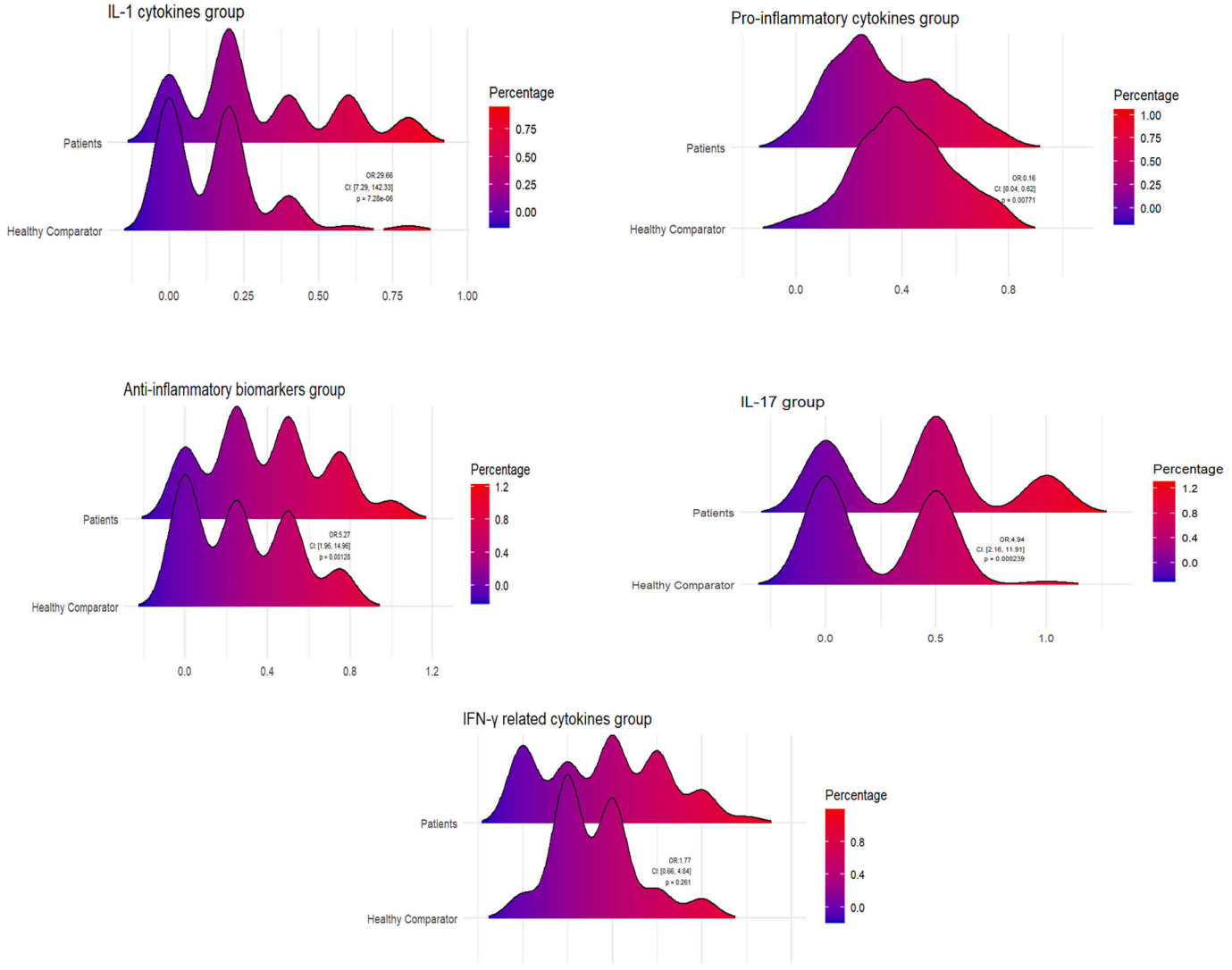

Fig. 3. Cytokine groups expression in PACS patients. Stacked bar plots represent the alterations among different cytokine groups between PACS patients and healthy comparators. The following cytokine or biomarker categories are shown: IL-1 cytokines, IL-17 cytokines, IFN-γ and IFN-γ–related cytokines, proinflammatory cytokines, and anti-inflammatory biomarkers. For each comparison, the odds ratio (OR), 95 % confidence intervals (CIs), and *p-value are displayed, calculated using ordinal regression. Abbreviations: IL: interleukin; IFNγ: Interferon γ; OR: Odds Ratio; CIs: Confidence intervals; n: number of patients.*

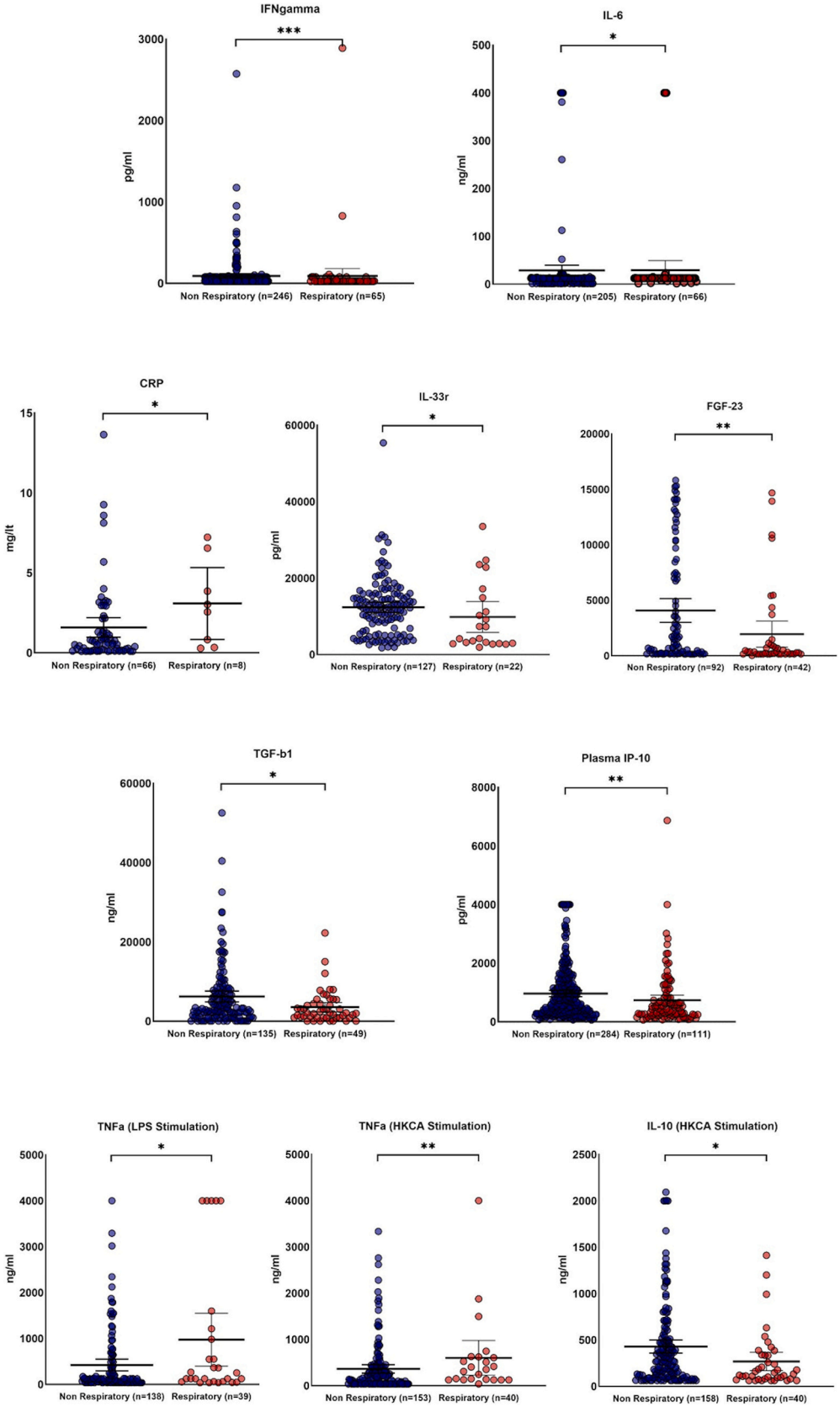

Fig. 4. Circulating mediators in patients with respiratory phenotype.. Concentrations of serum mediators and cytokines produced by stimulated PBMCs in patients with respiratory phenotype and other phenotypes of both the Discovery and Validation Cohort are shown. In all panels, lines represent the median of distribution and 95 % confidence intervals. The *p-values of comparisons by the Mann-Whitney U test are provided: * < 0.05; ** < 0.01; *** < 0.001; *** < 0.0001. Abbreviations: CRP, C-reactive protein; FGF: fibroblast growth factor; IFN: interferon; IL: interleukin; IP, interferon-gamma induced protein; TGF: transforming growth factor, TNF: tumor necrosis factor; LPS: lipopolysaccharide; HKCA: Heat-killed Candida albicans; n: number of patients.*

3.5. Transcriptome differences between PACS phenotypes

RNA expression was measured in 28 samples in total (11 with respiratory phenotype and 17 with a non-respiratory phenotype) from both Cohorts. After PCA, 1 outlier (LC210) was excluded that belonged to the non-respiratory group. Six differentially expressed genes (DEGs) were found (*LOC388588, AQP1, BAK1, COTL1, GRINA and TRPM2)* and were all up-regulated in patients with respiratory phenotype (Fig. 5A, Supplementary Table 14). The expression of these genes across the phenotypes and patients is shown in Fig. 5B.

To identify if molecular processes related to IL-1 and type-II interferons are enriched in patients with different PACS phenotypes and could be missed by applying arbitrary gene expression cutoffs, we performed GSEA Gene Ontology analysis comparing the gene expression profiles of samples derived from patients with the respiratory versus the non-respiratory phenotypes. Indeed, in accordance with the cytokines analysis, we found that responses to IL-1 and type-II interferons are enriched in patients with the respiratory phenotype compared to those with non-respiratory phenotypes (Supplementary Figure. 5).

3.6. Long-term changes of the epigenetic landscape of immune cells

We examined the epigenomic landscape of PBMCs from patients with respiratory-predominant symptoms ($n = 4$), asymptomatic patients ($n = 3$) and control samples (n = 4) by performing ChIP-seq experiments for H3K27ac, a marker of active enhancers and promoters [23]. Various quality control metrics confirmed the high quality of the datasets (Supplementary Table 15). We identified 41,717 H3K27ac regions (peaks) in total and performed differential peak calling between conditions using DESeq2 to identify condition-specific H3K27ac regions.

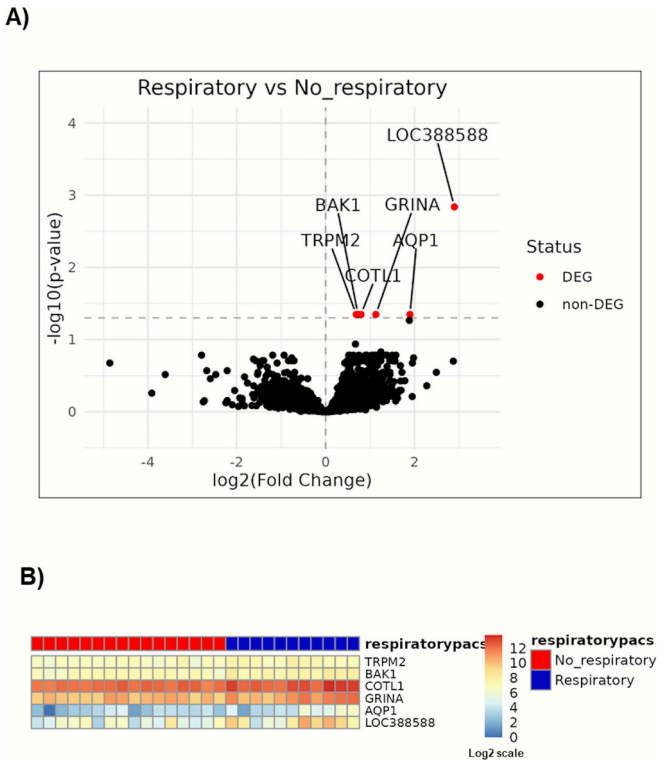

Fig. 5. Differentially Expressed Genes between PACS phenotypes.. (A) Volcano plot with the six differentially expressed genes (in red) identified between patients with respiratory ($n = 11$) *and non-respiratory phenotype ($n = 16$). All of them are up-regulated in the respiratory phenotype (DESeq2, log2 fold change cutoff = 0·5 and p-adj with false discovery rate < 0·05). (B) Heatmap presenting the raw expression levels of the differentially expressed genes across the phenotypes and patients.* Abbreviations: DEG, differentially expressed genes; LOC388588, SMIM1-Small Integral Membrane Protein 1; TRPM2, Transient Receptor Potential Cation Channel Subfamily M Member 2; BAK1, B-cell lymphoma 2 (BCL2) Antagonist/Killer 1; COTL1, Coactosin Like F-Actin Binding Protein 1; GRINA, Glutamate Ionotropic Receptor NMDA Type Subunit Associated Protein 1; AQP1, Aquaporin 1. (For interpretation of the references to colour in this figure legend, the reader is referred to the web version of this article.)

We found 413 and 320 regions with increased H3K27ac levels in respiratory-predominant patients and asymptomatic patients, respectively, while 71 regions had increased H3K27ac levels in both respiratory-predominant and asymptomatic samples compared to control samples (Fig. 6A, Supplementary Tables 16, 17, and 18). The genomic distribution analysis for regions with increased H3K27ac levels showed that approximately 50 % were inside gene bodies, about a quarter were found in intergenic regions, while there was also an enrichment for promoter regions (12–17 %) (Fig. 6B). The characteristic example of the *ZFP36L2* locus hosting multiple regions with increased H3K27ac levels in asymptomatic patients is presented in Fig. 6C. We also performed motif analysis for regions with increased H3K27ac levels in samples from Respiratory-predominant, Respiratory-predominant and Asymptomatic as well as in Asymptomatic-only samples and found an enrichment for the motif of the ETS family of transcription factors which are known regulators of myeloid and B-cells [24] in all three categories (Supplementary Figure. 6A-C). Finally, we discovered that regions with increased H3K27ac levels in asymptomatic patients were found in the vicinity of genes involved in immune-related processes, while no enriched ontologies were found for genes in the premises of respiratory-specific or common regions (Fig. 6D, Supplementary Tables 19, 20, and 21).

Concerning regions with decreased H3K27ac levels compared to control samples, we found 676 regions for respiratory-predominant samples and 541 regions for asymptomatic samples, while 171 regions had decreased H3K27ac in both respiratory-predominant and asymptomatic groups (Fig. 6E, Supplementary Tables 22, 23, 24). Their genomic distribution is presented in Fig. 6F. Motif analysis recovered the PU.1 and JUN family of motifs as enriched in samples from Respiratory predominant patients (Supplementary Figure. 6D), PU.1 in Respiratory-predominant and Asymptomatic (Supplementary Fig. 6E) and PU.1 and JUN family motifs for Asymptomatic-only regions (Supplementary Fig. 6F). Interestingly, the closest genes to all three categories of regions with decreased H3K27ac levels were related to immune processes (Fig. 6G, Supplementary Tables 25, 26, 27). Characteristic examples include *CCL2, IL1A, NFKB1,* and *NFKBIA,* which had regions with decreased H3K27ac levels in both respiratory-predominant and asymptomatic samples, *OASL* and *CCL5* for respiratory-predominant samples, and *GBP5, GBP6,* and *IL1B* for asymptomatic samples.

4. Discussion

In the present study, we sought to shed light on PACS phenotypes and particularly their association with immune dysfunction and alterations in gene expression and active DNA regulatory elements. Firstly, we found a significant immune dysregulation of cytokine network post-COVID represented by abnormal concentrations of the circulating cytokines and mediators that persist for months after recovery from the initial COVID-19 pneumonia. Secondly, in patients meeting the WHO criteria for PACS, we were able to discern five clinical phenotypes. Finally, in a subset of patients, we assessed alterations in the whole transcriptome (using RNA-seq) as well as markers of active DNA regulatory elements (using H3K27ac ChIP-seq) that could underlie the immune dysregulation.

Post-acute sequelae of SARS-CoV-2 infection include a wide variety of symptoms and signs that abide, worsen or re-emerge following the acute phase of the infection. Our analysis reveals a significantly higher number of patients experiencing PACS symptoms compared to other studies [25]. Two main explanations can be provided: a) most of study participants were hospitalized for COVID-19 pneumonia and this may

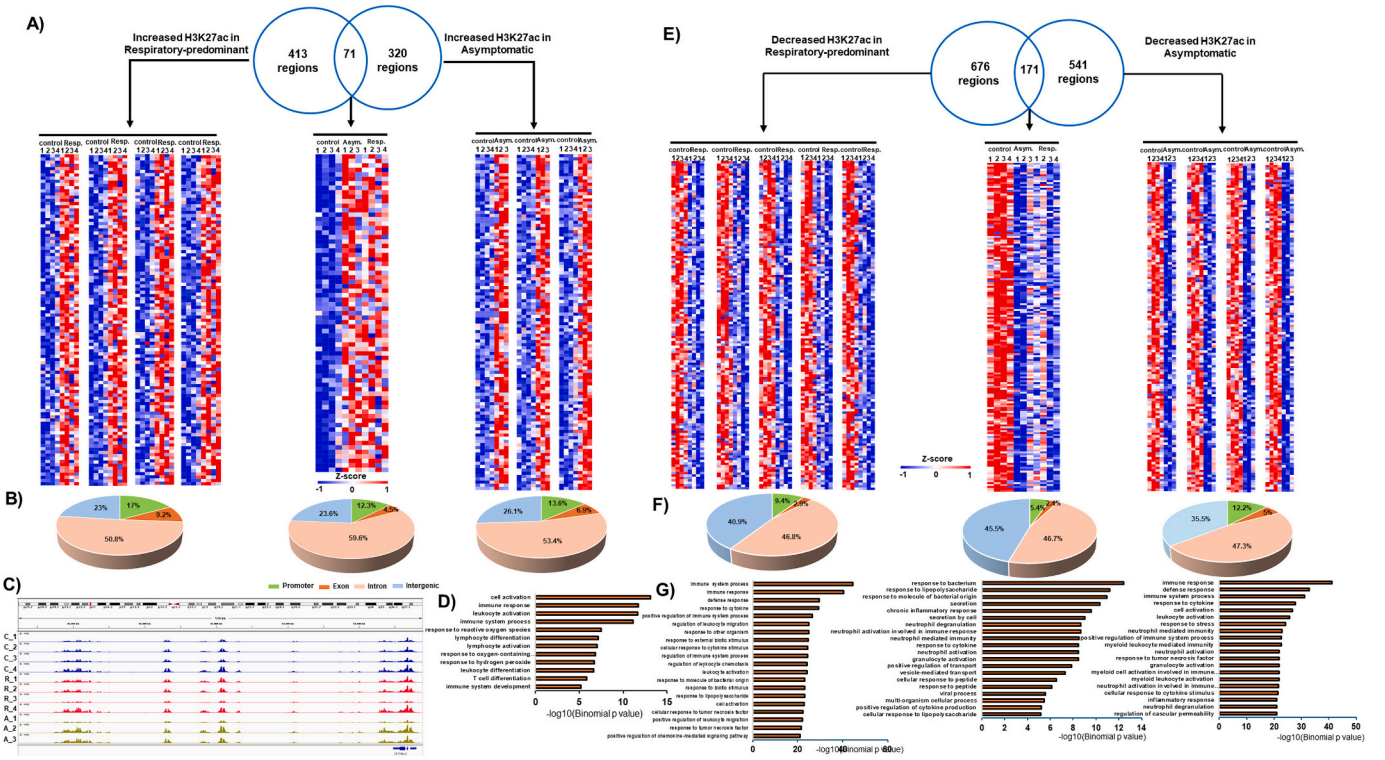

Fig. 6. Alterations in H3K27ac levels of active DNA regulatory elements between patients with different PACs phenotypes.. (A) Venn diagram showing regions with increased H3K27ac levels in respiratory-predominant patients and asymptomatic patients, as well as regions with increased H3K27ac in both groups of samples compared to controls. The heatmaps below depict the above-mentioned regions. (B) The genomic distribution of regions with increased H3K27ac levels in respiratory-predominant patients and asymptomatic patients as well as regions with increased H3K27ac in both groups of samples compared to controls. (C) IGV browser snapshot depicting H3K27ac levels for a characteristic locus hosting multiple regions with increased H3K27ac levels in the vicinity of the *ZFP36L2 gene in samples from asymptomatic patients. (D) Gene ontology analysis for the closest genes to regions with increased H3K27ac levels in samples from asymptomatic patients revealed immune-related processes as enriched. (E) Venn diagram showing regions with decreased H3K27ac levels in respiratory-predominant patients and asymptomatic patients, as well as regions with decreased H3K27ac in both groups of samples compared to controls. The heatmaps below depict the above-mentioned regions. (F) The genomic distribution of regions with decreased H3K27ac levels in respiratory-predominant patients and asymptomatic patients as well as regions with decreased H3K27ac in both groups of samples compared to controls. (G) Gene ontology analysis for the closest genes to regions with decreased H3K27ac levels revealed immune-related processes as enriched in all three categories.*

drive more severe PACS; and b) patient selection was based on a questionnaire used in a former registrational clinical trial [5] which may be more sensitive.

Dexamethasone treatment during the acute phase of COVID-19 has been described to prevent the progression to PACS [26], whereas antiviral treatment has had mixed results regarding its impact [27]. The analysis of the 90-day outcome of the SAVE-MORE trial participants described that anakinra treatment during the acute phase of the disease was followed by fewer sequelae [28]. Furthermore, in our study, treatment with anakinra during acute COVID-19 pneumonia seems to also prevent from developing the respiratory phenotype of PACS. Future clinical trials need to assess whether anakinra administered during the chronic phase of PACS can similarly ameliorate respiratory symptoms.

The seemingly contradictory combination of anti-inflammatory upregulation and pro-inflammatory down-regulation of immune biomarkers in our results is compatible with a chronically adjusted, tolerance-like immune profile after severe viral infection [29,30]. Although it is anticipated that pro-inflammation should prevail in PACS because of the high incidence of fatigue, previous research in patients with chronic fatigue syndrome before the pandemic suggests similar dissociation between immune patterns. In a randomized clinical trial, treatment patients with chronic fatigue conditions with the IL-1 blocker anakinra did not result in reduction of fatigue severity [31], suggesting that chronic fatigue is not a pro-inflammatory condition.

The expressions of *COTL1*, *TRPM2*, *BAK1* and *AQP1* were upregulated among patients with respiratory PACS. These genes encode for proteins associated with the maturation of IL-1 across different cellular environments and experimental models [32–35]. This is compatible with the over-activation of the IL-1 cytokine group in patients with respiratory PACS.

The ChIP-seq experiments against H3K27ac, a marker of active enhancers and promoters, revealed regions with altered enhancer activity (H3K27ac levels) in PACS phenotypes, hosting motifs for immune cell regulators and found in the vicinity of genes associated with various immune processes. Moreover, specifically, regions with altered H3K27ac levels hosted motifs for major regulators of immune responses such as PU.1 and Jun family members and were found in the proximity of characteristic immune response genes such as *CCL2, CCL5, IL1A, NFKB1, NFKBIA* and *OASL*. These genes encode for cytokine production which is increased respiratory PACS. Overall results suggest that COVID-19 infection leaves a long-standing impact/imprint on the host immune epigenetic landscape. Nevertheless, changes in enhancer activity were rather limited in magnitude and extent between patient groups involving approximately 2 % of the totality of putative enhancers. This could reflect the well-established inter-individual variability in immune responses [36] or could indicate that other epigenomics marks, such as histone and DNA methylation, could serve as a reservoir of epigenetic memory. Moreover, other unexplored sources of variation beyond epigenetic state could also contribute to the altered cytokine release capacity of PBMCs upon stimulation.

We would like to acknowledge certain limitations of our study. First, we were unable to perform lung function tests in all patients of the study.

Hence, PACS phenotyping relied mainly on the subjective responses of patients to questionnaires. A second limitation was that transcriptomic and epigenomic analyses were performed only for a subset of patients.

To conclude, long-term immune changes post COVID-19 are heterogeneous, and different pathways appear to be linked to specific clinical phenotypes.

Ethics aproval statement

Exploratory Cohort of 2020 was run under approval of the protocol ESPACE (EudraCT number 2020–001039-29; Clinicaltrials.gov NCT04339712); the remaining study run under approvals by the Ethics Committee of the participating hospitals (Attikon University Hospital 11/1/2022; General Hospital of Piraeus Tzaneio 14/5/2021; Sotiria General Hospital of Chest Diseases-3rd University Department of Internal Medicine 28/3/2022; Sotiria General Hospital of Chest Diseases-1st University Pulmonary Medicine Department 28/3/2022, Thriasio General Hospital 13/4/2022; Ospedale Policlinico San Martino 2/5/2022; IRCCS Lazzaro Spallanzani 14/7/2022; Policlinico Universitario Agostino Gemelli 3/3/2022; Spedali civili 5/4/2022; Ospedale Sacro Cuore Don Calabria 23/2/2022; IRCCS San Raffaele 11/5/2022; Ospedale di Jesolo-Unità Operativa Malattie Infettive 15/3/2022; Ospedale Maggiore Policlinico 12/4/2022; Hospital Clínic de Barcelona 10/6/2022). All patients or their legal representatives provided written informed consent before enrollment.

Authors contributions

CS contributed in patients' recruitment and clinical assessment and collection of clinical data, drafted the manuscript and gave approval for the submitted version.

EJG-B conceptualized the study, analyzed the data, takes full responsibility for data integrity, drafted the manuscript and gave approval for the submitted version.

GP, EK, ET, EG, AS, MT, EC, VR, NR, NI, EN, ET, AA, MB, LD, AT, GA, CD, KL, NC, PC, AG, PP, KS, KI, FSS, MP, PDV, LS, AB, AB, SS and HM enrolled patients in the clinical study, collected clinical data, critically revised the manuscript for intellectual content and gave approval for the submitted version.

HF and LE collected clinical data and critically revised the manuscript for intellectual content and gave approval for the submitted version.

VE performed lung function tests, critically revised the manuscript for intellectual content and gave approval for the submitted version.

GD and PK performed cytokine measurements and PBMCs experiments, critically revised the manuscript for intellectual content and gave approval for the submitted version.

SF, GV, DT, ES, AZ and RtH performed and analyzed RNA-seq and ChIP-seq experiments, critically revised the manuscript and gave approval for the submitted version.

Funding

The trial was sponsored by the Hellenic Institute for the Study of Sepsis (HISS) and funded in part by HISS and in part by Swedish Orphan Biovitrum AB (Sobi). HISS was responsible for the study design, study conduct, analysis and interpretation of data, and decision to publish. Sobi had no role in study design, data collection, data analysis, data interpretation, or writing of the report.

CRediT authorship contribution statement

Chrysanthi Sidiropoulou: Writing – original draft, Visualization, Investigation. **Garyphallia Poulakou:** Writing – review & editing, Investigation. **Evdoxia Kyriazopoulou:** Writing – review & editing, Investigation. **Elisavet Tasouli:** Writing – review & editing, Investigation. **Efthymia Giannitsioti:** Writing – review & editing, Investigation. **Anna Strikou:** Writing – review & editing, Investigation. **Maria Tsilika:** Investigation. **Eirini Christaki:** Writing – review & editing, Investigation. **Vassiliki Rapti:** Writing – review & editing, Investigation. **Vassiliki Evangelopoulou:** Writing – review & editing, Investigation. **Nikoletta Rovina:** Writing – review & editing, Investigation. **Nathalie Iannotti:** Writing – review & editing, Investigation. **Emanuele Nicastri:** Writing – review & editing, Investigation. **Eleonora Taddei:** Writing – review & editing, Investigation. **Helena Florou:** Writing – review & editing, Project administration. **Andrea Angheben:** Writing – review & editing, Investigation. **Matteo Bassetti:** Writing – review & editing, Investigation. **Lorenzo Dagna:** Writing – review & editing, Investigation. **Antonio Torres:** Writing – review & editing, Investigation. **Spyros Foutadakis:** Writing – original draft, Formal analysis. **George Adamis:** Writing – review & editing, Investigation. **Emmanouil Stylianakis:** Writing – original draft, Formal analysis. **Giannis Vatsellas:** Writing – review & editing, Investigation. **Georgia Damoraki:** Writing – review & editing, Investigation. **Leda Efstratiou:** Writing – review & editing, Project administration. **Christina Damoulari:** Writing – review & editing, Investigation. **Konstantinos Leventogiannis:** Writing – review & editing, Investigation. **Achilleas Laskaratos:** Writing – review & editing, Investigation. **Panagiotis Koufargyris:** Writing – review & editing, Investigation. **Nikoletta Charalampaki:** Writing – review & editing, Investigation. **Paraskevi Chra:** Writing – review & editing, Investigation. **Aglaia Galanopoulou:** Writing – review & editing, Investigation. **Dimitris Thanos:** Writing – review & editing, Investigation. **Periklis Panagopoulos:** Writing – review & editing, Investigation. **Konstantinos Syrigos:** Writing – review & editing, Investigation. **Athanasios Ziogas:** Writing – review & editing, Investigation. **Rob ter Horst:** Writing – review & editing, Validation. **Jos W.M. van der Meer:** Writing – review & editing, Validation. **Konstantina Iliopoulou:** Writing – review & editing, Investigation. **Francesco Saverio Serino:** Writing – review & editing, Investigation. **Maria Pavlaki:** Writing – review & editing, Investigation. **Pierluigi Del Vecchio:** Writing – review & editing, Investigation. **Laura Scorzolini:** Writing – review & editing, Investigation. **Alessandra Bandera:** Writing – review & editing, Investigation. **Agamemnon Bakakos:** Writing – review & editing, Investigation. **Styliani Sympardi:** Writing – review & editing, Investigation. **Haralampos Milionis:** Writing – review & editing, Investigation. **Mihai G. Netea:** Writing – review & editing, Validation. **Evangelos J. Giamarellos-Bourboulis:** Writing – review & editing, Writing – original draft, Supervision, Resources, Methodology, Funding acquisition, Formal analysis, Data curation, Conceptualization.

Declaration of competing interest

GP has received honoraria and/or consulting fees by Astra-Zeneca, Gilead, GSK, Menarini, MSD, Norma, Pfizer and SOBI and research grants by the University of Minnesota/University College London, the Hellenic Institute for the Study of Sepsis, Bausch, Roche, Xenothera, FabNTech and Pfizer.

HM reports receiving honoraria, consulting fees and non-financial support from healthcare companies, including Amgen, Angelini, Bayer, Mylan, MSD, Pfizer, and Servier.

MGN is a scientific founder of TTxD, Biotrip and Lemba and was supported by an ERC Advanced Grant (#833247) and a Spinoza grant of the Netherlands Organization for Scientific Research.

EJG-B reports honoraria from Abbott Products Operations, bioMérieux, Brahms GmbH, InflaRx GmbH, and Swedish Orphan Biovitrum AB (granted to the National and Kapodistrian University of Athens); independent educational grants from Abbott Products Operations, bioMérieux Inc., Entegrion, MSD, and Swedish Orphan Biovitrum AB (granted to the Hellenic Institute for the Study of Sepsis) and from AbbVie, InCyte, MSD, Novartis, UCB and Sanofi (granted to the National and Kapodistrian University of Athens); and funding from the Horizon 2020 European Grants ImmunoSep and RISCinCOVID and the Horizon

Health grants EPIC-CROWN-2, POINT and Homi-Lung (granted to the Hellenic Institute for the Study of Sepsis).

The other authors do not declare any conflict of interest.

Appendix A. Supplementary data

Supplementary data to this article can be found online at https://doi.org/10.1016/j.clim.2025.110656.

Data availability

Raw data are available for download from the server of the Hellenic Institute for the Study of Sepsis (https://wshiss.com/). Username and Password are provided upon request from the corresponding author at egiamarel@med.uoa.gr

References

[1] J.B. Soriano, S. Murthy, J.C. Marshall, P. Relan, J.V. Diaz, A clinical case definition of post-COVID-19 condition by a Delphi consensus, Lancet Infect. Dis. 22 (4) (2022) e102–e107, https://doi.org/10.1016/S1473-3099(21)00703-9.
[2] K. Yin, M.J. Peluso, X. Luo, et al., Long COVID manifests with T cell dysregulation, inflammation and an uncoordinated adaptive immune response to SARS-CoV-2, Nat. Immunol. 25 (2) (2024) 218–225, https://doi.org/10.1038/s41590-023-01724-6.
[3] World Health Organization, Coronavirus Disease (COVID-19): Post COVID-19 Condition, Available from, https://www.who.int/news-room/questions-and-answers/item/coronavirus-disease-(covid-19)-post-covid-19-condition, 2021 (Accessed 25 July 2025).
[4] S. Wulf Hanson, C. Abbafati, J.G. Aerts, et al., Global Burden of Disease Long COVID Collaborators, Estimated global proportions of individuals with persistent fatigue, cognitive, and respiratory symptom clusters following symptomatic COVID-19 in 2020 and 2021, JAMA 328 (16) (2022) 1604–1615, https://doi.org/10.1001/jama.2022.18931.
[5] E. Kyriazopoulou, G. Poulakou, H. Milionis, et al., Early treatment of COVID-19 with anakinra guided by soluble urokinase plasminogen receptor plasma levels: a double-blind, randomized controlled phase 3 trial, Nat. Med. 27 (10) (2021) 1752–1760, https://doi.org/10.1038/s41591-021-01499-z.
[6] V.-T. Tran, C. Riveros, B. Clepier, et al., Development and validation of the long coronavirus disease (COVID) symptom and impact tools: a set of patient-reported instruments constructed from patients' lived experience, Clin. Infect. Dis. 74 (2) (2022) 278–287, https://doi.org/10.1093/cid/ciab352.
[7] E. Afgan, D. Baker, B. Batut, et al., The galaxy platform for accessible, reproducible and collaborative biomedical analyses: 2018 update, Nucleic Acids Res. 46 (W1) (2018) W537–W544, https://doi.org/10.1093/nar/gky379.
[8] Posit team, RStudio: Integrated Development Environment for R, Posit Software, PBC, Boston, MA, 2024. Available from, https://posit.co/ (Accessed 25 July 2025).
[9] D. Kim, J.M. Paggi, C. Park, C. Bennett, S.L. Salzberg, Graph-based genome alignment and genotyping with HISAT2 and HISAT-genotype, Nat. Biotechnol. 37 (8) (2019) 907–915, https://doi.org/10.1038/s41587-019-0201-4.
[10] S. Anders, P.T. Pyl, W. Huber, HTSeq—a Python framework to work with high-throughput sequencing data, Bioinformatics 31 (2) (2015) 166–169, https://doi.org/10.1093/bioinformatics/btu638.
[11] M.I. Love, W. Huber, S. Anders, Moderated estimation of fold change and dispersion for RNA-seq data with DESeq2, Genome Biol. 15 (12) (2014) 550, https://doi.org/10.1186/s13059-014-0550-8.
[12] Y. Liao, J. Wang, E.J. Jaehnig, Z. Shi, B. Zhang, WebGestalt 2019: gene set analysis toolkit with revamped UIs and APIs, Nucleic Acids Res. 47 (W1) (2019) W199–W205, https://doi.org/10.1093/nar/gkz401.
[13] B. Langmead, S.L. Salzberg, Fast gapped-read alignment with bowtie 2, Nat. Methods 9 (4) (2012) 357–359, https://doi.org/10.1038/nmeth.1923.
[14] H. Li, B. Handsaker, A. Wysoker, et al., The sequence alignment/map format and SAMtools, Bioinformatics 25 (16) (2009) 2078–2079, https://doi.org/10.1093/bioinformatics/btp352.
[15] Y. Zhang, T. Liu, C.A. Meyer, et al., Model-based analysis of ChIP-seq (MACS), Genome Biol. 9 (9) (2008) R137, https://doi.org/10.1186/gb-2008-9-9-r137.
[16] A.R. Quinlan, I.M. Hall, BEDTools: a flexible suite of utilities for comparing genomic features, Bioinformatics 26 (6) (2010) 841–842, https://doi.org/10.1093/bioinformatics/btq033.
[17] F. Ramírez, F. Dündar, S. Diehl, B.A. Grüning, T. Manke, deepTools: a flexible platform for exploring deep-sequencing data, Nucleic Acids Res. 42 (W1) (2014) W187–W191, https://doi.org/10.1093/nar/gku365.
[18] C.Y. McLean, D. Bristor, M. Hiller, et al., GREAT improves functional interpretation of cis-regulatory regions, Nat. Biotechnol. 28 (5) (2010) 495–501, https://doi.org/10.1038/nbt.1630.
[19] H. Shin, et al., CEAS: cis-regulatory element annotation system, Bioinformatics 25 (19) (2009) 2605–2606, https://doi.org/10.1093/bioinformatics/btp479.
[20] T. Liu, J.A. Ortiz, L. Taing, et al., Cistrome: an integrative platform for transcriptional regulation studies, Genome Biol. 12 (8) (2011) R83, https://doi.org/10.1186/gb-2011-12-8-r83.
[21] P. Machanick, T.L. Bailey, MEME-ChIP: motif analysis of large DNA datasets, Bioinformatics 27 (12) (2011) 1696–1697, https://doi.org/10.1093/bioinformatics/btr189.
[22] R. Zheng, C. Wan, S. Mei, et al., Cistrome data browser: expanded datasets and new tools for gene regulatory analysis, Nucleic Acids Res. 47 (D1) (2019) D729–D735, https://doi.org/10.1093/nar/gky1094.
[23] E. Calo, J. Wysocka, Modification of enhancer chromatin: what, how, and why? Mol. Cell 49 (5) (2013) 825–837, https://doi.org/10.1016/j.molcel.2013.01.038.
[24] M. Leddin, C. Perrod, M. Hoogenkamp, et al., Two distinct auto-regulatory loops operate at the PU.1 locus in B cells and myeloid cells, Blood 117 (10) (2011) 2827–2838, https://doi.org/10.1182/blood-2010-08-302976.
[25] R.S. Peter, A. Nieters, H.G. Kräusslich, et al., Post-acute sequelae of covid-19 six to 12 months after infection: population based study, BMJ 379 (2022) e071050, https://doi.org/10.1136/bmj-2022-071050.
[26] D. Badenes Bonet, O.A. Caguana Vélez, X. Duran Jordà, et al., Treatment of COVID-19 during the acute phase in hospitalized patients decreases post-acute sequelae of COVID-19, J. Clin. Med. 12 (13) (2023) 4158, https://doi.org/10.3390/jcm12124158.
[27] O.P.O. Nevalainen, S. Horstia, S. Laakkonen, et al., Effect of remdesivir post hospitalization for COVID-19 infection from the randomized SOLIDARITY Finland trial, Nat. Commun. 13 (1) (2022) 6152, https://doi.org/10.1038/s41467-022-33825-5.
[28] K. Akinosoglou, A. Kotsaki, I.M. Gounaridi, et al., Efficacy and safety of early soluble urokinase plasminogen receptor plasma-guided anakinra treatment of COVID-19 pneumonia: a subgroup analysis of the SAVE-MORE randomised trial, EClinicalMedicine 56 (2023) 101785, https://doi.org/10.1016/j.eclinm.2022.101785.
[29] M.J. Peluso, S.G. Deeks, Mechanisms of long COVID and the path toward therapeutics, Cell 187 (20) (2024) 5500–5529, https://doi.org/10.1016/j.cell.2024.07.054.
[30] W.J. Wiersinga, T. van der Poll, Immunopathophysiology of human sepsis, EBioMedicine 86 (2022) 104363, https://doi.org/10.1016/j.ebiom.2022.104363.
[31] M.E. Roerink, S.J.H. Bredie, M. Heijnen, et al., Cytokine inhibition in patients with chronic fatigue syndrome: a randomized trial, Ann. Intern. Med. 166 (8) (2017) 557–564, https://doi.org/10.7326/M16-2391.
[32] J. Zhang, H. Jiang, Knockdown of BATF alleviates lung injury in septic neonates through transcriptional regulation of COTL1, Cent. Eur. J. Immunol. 49 (3) (2024) 238–251, https://doi.org/10.5114/ceji.2024.144865.
[33] X. Li, W. Wang, Y. Shao, et al., LncTRPM2-AS inhibits TRIM21-mediated TRPM2 ubiquitination and prevents autophagy-induced apoptosis of macrophages in asthma, Cell Death Dis. 12 (12) (2021) 1153, https://doi.org/10.1038/s41419-021-04437-6.
[34] D. Chauhan, E. Bartok, M.M. Gaidt, et al., BAX/BAK-induced apoptosis results in caspase-8-dependent IL-1β *maturation in macrophages*, Cell Rep. 25 (9) (2018) 2354–2368.e5, https://doi.org/10.1016/j.celrep.2018.10.087.
[35] V. Rabolli, L. Wallemme, S. Lo Re, et al., Critical role of aquaporins in interleukin 1β (IL-1β)-induced inflammation, J. Biol. Chem. 289 (20) (2014) 13937–13947, https://doi.org/10.1074/jbc.M113.534594.
[36] K.A. Aracena, Y.-L. Lin, K. Luo, et al., Epigenetic variation impacts individual differences in the transcriptional response to influenza infection, Nat. Genet. 56 (3) (2024) 408–419, https://doi.org/10.1038/s41588-024-01668-z.